THE ASTROPHYSICAL JOURNAL, 282:135–141, 1984 July 1

SPECTROPHOTOMETRY OF YOUNG SUPERNOVA REMNANTS

MICHAEL A. DOPITA AND IAN R. TUOHY
Mount Stromlo and Siding Spring Observatories, Research School of Physical Sciences, Australian National University
Received 1983 August 24; accepted 1983 December 28

ABSTRACT

Spectrophotometric data are presented for four young oxygen-rich supernova remnants: G292.0+1.8 in the Galaxy, N132D and 0540−69.3 in the Large Magellanic Cloud, and 1E 0102.2−7219 in the Small Magellanic Cloud. Although these data are insufficient to derive unique physical conditions and chemical abundances in the remnants, they serve to show that a common physical process is responsible for the excitation in all four remnants.

We also derive sensitive upper limits on emission from elements other than oxygen and neon from global spectra of N132D and 1E 0102.2−7219 of very high signal-to-noise ratio, and show that 0540−69.3 is peculiar in its chemical composition, probably resulting from optical excitation of material from the innermost zones of the ejecta from a massive precursor star.

Subject headings: galaxies: Magellanic Clouds — nebulae: abundances — nebulae: supernova remnants — spectrophotometry

I. INTRODUCTION

In several young supernova remnants (SNR), fast-moving material has been identified at optical wavelengths, which to the limits of observational measurement, appears to be both totally devoid of hydrogen or helium and grossly overabundant in oxygen. The first discovered and most intensively studied example of this phenomenon is the system of fast-moving knots (FMK) in Cas A, for many of which there are spectrophotometric and radial velocity data (Peimbert 1971; Chevalier and Kirshner 1978, 1979) and also proper motion information (van den Bergh and Dodd 1970; Kamper and van den Bergh 1976). More recently, a further example of this class of object has been found in the southern skies, G292.0+1.8 (Goss *et al.* 1979; Murdin and Clark 1979). Several extragalactic examples are now also known; in the Large Megallanic Cloud N132D (Danziger and Dennefeld 1976*a*, *b*; Lasker 1978, 1980) and 0540−69.3 (Mathewson *et al.* 1980), and in the Small Magellanic Cloud 1E 0102.2−7219 (Dopita, Tuohy, and Mathewson 1981; Tuohy and Dopita 1983). An extraordinary bright and dense example was discovered in NGC 4449 (Balick and Heckman 1978), and this has since been observed in some detail (Kirshner and Blair 1980; Blair, Kirshner, and Winkler 1983).

The balance of evidence on these oxygen-rich SNRs strongly supports the idea that we are seeing fragments of massive precursor stars which have undergone very little interaction with the interstellar medium (ISM) since the supernova event. Thus, if we can correctly interpret the spectra of such regions, we may expect to derive a wealth of information on nucleosynthesis in massive stars both before and during the supernova explosion, and on the role of these objects in the chemical evolution of galaxies.

In this paper we present new spectrophotometric data on the Magellanic Cloud examples and on G292.0+1.8, and we investigate the extent to which we can derive information on chemical abundances and physical conditions in these remnants. We test the hypothesis that the visible emission is a consequence of radiative shock waves propagating into dense cloudlets of stellar ejecta in a separate paper (Dopita, Binette, and Tuohy 1984).

II. OBSERVATIONS

The optical spectra were obtained under photometric conditions at the 3.9 m Anglo-Australian Telescope during several observing runs in the period 1981–1983. The Royal Greenwich Observatory spectrograph was used with its 25 cm camera and the Image Photon-Counting System (IPCS; Boksenberg 1972) as detector. A grating of 250 l mm^{-1} blazed in the blue was used in the first order with a slit width of 300 μm (2″.0 on the sky), giving a spectral resolution of 9 Å, and a useful spectral coverage of 3200–7400 Å. The external memory was used to give 58 spectra, each 2040 pixels long, and each separated by 2″.07 on the sky.

The grating has no measurable second-order leak (much less than 5%), so the following reduction procedure could be used to give flux calibrated spectra. First, pixel to pixel variations were removed by the division of the data by a normalized flat field obtained by a long exposure of a tungsten lamp, unfiltered, in the third-order red. Second, each spectrum was rebinned and made linear in wavelength by using a two-dimensional fourth-order polynomial fit to the calibration arcs. Third, the mean of those spectra adjudged to be free of nebular or stellar contributions was subtracted from each spectrum to cancel sky emission. Fourth, the spectra were converted to flux by correcting for atmospheric extinction and by multiplying by a smooth response function derived from observations of white dwarf standard stars (Oke 1974).

In order to give the most accurate spectrophotometry, we have selected knots in each remnant characterized by high surface brightness and low velocity dispersion. Thus the results given in Table 2, corresponding to the slit positions in Table 1, may not be representative of the remnants as a whole, as both physical conditions and elemental abundances may vary from knot to knot. The blue portions of a typical pair of spectra of 1E 0102.2−7219 in the SMC are shown in Figure 1. Note the difference in the [O II]/[O III] line ratios, which although

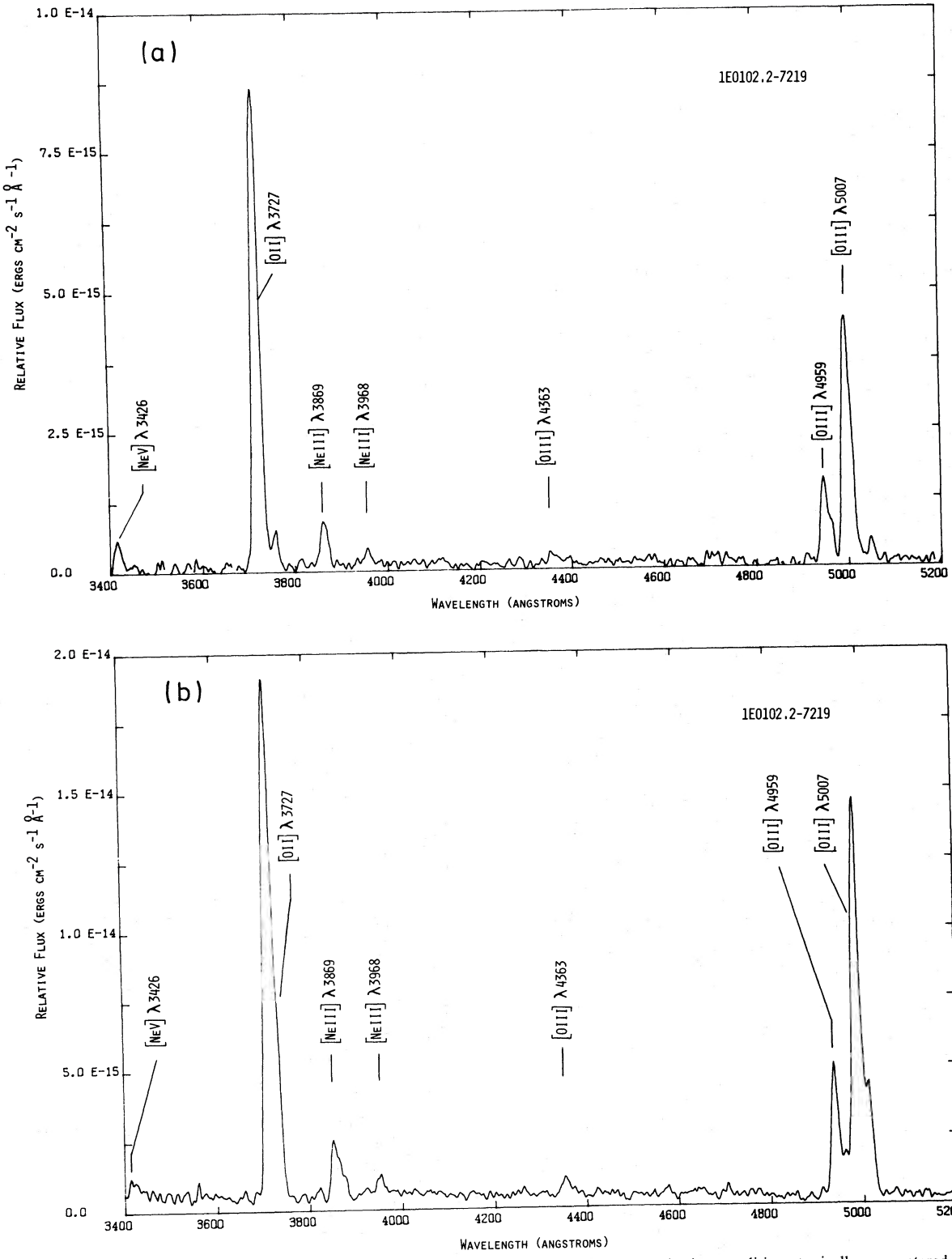

FIG. 1.—Moderate resolution blue spectra of 1E 0102.2−7219 in the SMC showing the range of excitation conditions typically encountered in the SNRs we observed. Slit centers and position angles were $01^h02^m24^s.1$, $-72°18'05''$, 270° (Fig. 1*a*) and $01^h02^m24^s.0$, $-72°18'13''$, 270° (Fig. 1*b*).

TABLE 1

SLIT PARAMETERS[a]

SNR	Right Ascension (1950)	Declination (1950)	Position Angle (degrees)
G292.0+1.8	$11^h22^m27^s.9$	$-58°59'32''$	350
0540−69.3	05 40 31.0	−69 21 26	180
N132D	05 25 29.1	−60 40 44	180
0102.2−7219	01 02 24.0	−72 18 13	270

[a] Slit centers and position angles correspond to the measurements presented in Table 2.

marked, is not enormous. This is representative of the range observed within a given remnant and is in contrast with the enormous variations in spectra observed within the FMK of Cas A (Kirshner and Chevalier 1977; Chevalier and Kirshner 1978, 1979), much of which can be ascribed to compositional variations.

In the case of N132D and 1E 0102.2−7219 we have been able to extract global mean spectra from further long slit observations covering the full extent of the oxygen-emitting material in both remnants. The data for N132D were acquired at medium resolution (~4 Å FWHM) in the wavelength range 3400–5100 Å, while the 1E 0102.2−7219 spectra were those used to produce the velocity map of Tuohy and Dopita (1983) and span the range 3200–7400 Å with a resolution of ~8 Å FWHM. If the set of ~100 spectra for each remnant had simply been added together, the substantial velocity shifts would have smeared the lines into broad profiles even though the individual spectra show quite narrow velocity spreads. We have therefore subjected the data to the following procedure. First, a subset of ~60 spatial elements for each remnant were selected on the basis of good signal-to-noise ratios and low velocity dispersion. The spectra of these spatial elements were then cross-correlated against a template spectrum to establish the velocity shifts within the individual spectra. After correcting each spectrum to a rest velocity system the 60 spectra were co-added to produce the composite spectra shown in Figures 2 and 3. These spectra of N132D and 1E 0102.2−7219 have the highest signal-to-noise ratio yet achieved, since to obtain comparable signal on a single spectrum would require ~20 hours of observation.

TABLE 3

GLOBAL SPECTRA OF N132D AND 1E 0102.2 − 7219

ION	λ(Å)	FLUX RELATIVE TO I5007 = 100.0 N132D	1E 0102.2−7219
[Ne III], [Ne V]	3343, 46	...	6.3 ± 0.9[a]
[Ne V]	3426	<0.9	9.5 ± 0.5
?	~3540	...	1.8 ± 0.2
[O II]	3726, 29	165 ± 1.0	199 ± 2
[Ne III]	3869	8.3 ± 0.2	17.2 ± 0.2
Ca II	3933	<0.5	<0.7
[Ne III]	3968	3.0 ± 0.2	3.8 ± 0.2
[S II]	4069, 76	<0.5	<0.4
C II	4267	<0.5	<0.4
[O III]	4363	4.7 ± 0.2	4.6 ± 0.2
Mg I]	4571	<0.4	<0.4
He II	4686	<0.5	<0.4
[Ar IV]	4711, 40	<0.4	<0.8
[Ne IV]	4725	<0.4	1.4 ± 0.2[a]
Hβ	4861	<0.5	[b]
[O III]	4959	31.1 ± 0.8	32.0 ± 1.6
[O III]	5007	100.0	100.0
[O I]	6300	...	5.0 ± 0.3
[O II]	7319	...	~4

[a] Blend.

[b] No measurement possible due to imperfect subtraction of diffuse Hβ.

We find it interesting that despite the much improved detection limit, no new emission lines were found for N132D. For 1E 0102.2−7219, however, the following weak features appear in the global spectrum: a blend near λ3346 corresponding to [Ne III] λ3343 and [Ne V] λ3346, emission from [Ne IV] λ4725, and an as yet unidentified feature near λ3540. In Table 3 we give the relative intensities of the oxygen and neon lines with the measurement errors and 3 σ upper limits for other selected lines that might have been expected for the two remnants. In general, 3 σ upper limits of 0.5 and 0.4 apply for N132D and 1E 0102.2−7219, respectively, to any other lines not specifically mentioned in the table (within the observed wavelength range).

TABLE 2

SPECTROPHOTOMETRY OF YOUNG SNRs

ION	λ(Å)	OBSERVED FLUX RELATIVE TO I5007 = 100.0 G292.0+1.8	0540−69.3	N132D	1E 0102.2−7219
[Ne V]	3425.9	...	...	...	3.5
[O II]	3726.1, 3728.8	79.0 ± 1.8	54.2 ± 2.0	205 ± 3.5	130 ± 1.8
[Ne III]	3868.8	6.9	...	9.1	14.0
	3967.5	2.3	...	2.8	4.9
[S II]	4068.6, 4076.4	...	4.0	...	...
[O III]	4363.2	3.4 ± 1.0	3.2 ± 1.3	4.4 ± 1.4	4.3 ± 1.3
	4958.9	31.9	30.2	33.9	33.8
	5006.9	100	100	100	100
[O I]	6300.3	(5)	2.9	10.9	2.9
	6363.8	...	1.1	3.6	(1.0)
Ca I]	6572.8	...	17.4	...	...
[S II]	6716.4, 6730.8	...	63.5 ± 5.0	...	...
[O II]	7319, 7330	<10	(2)	10.4 ± 3.0	...

NOTE.—Values in parentheses denote uncertain measurements.

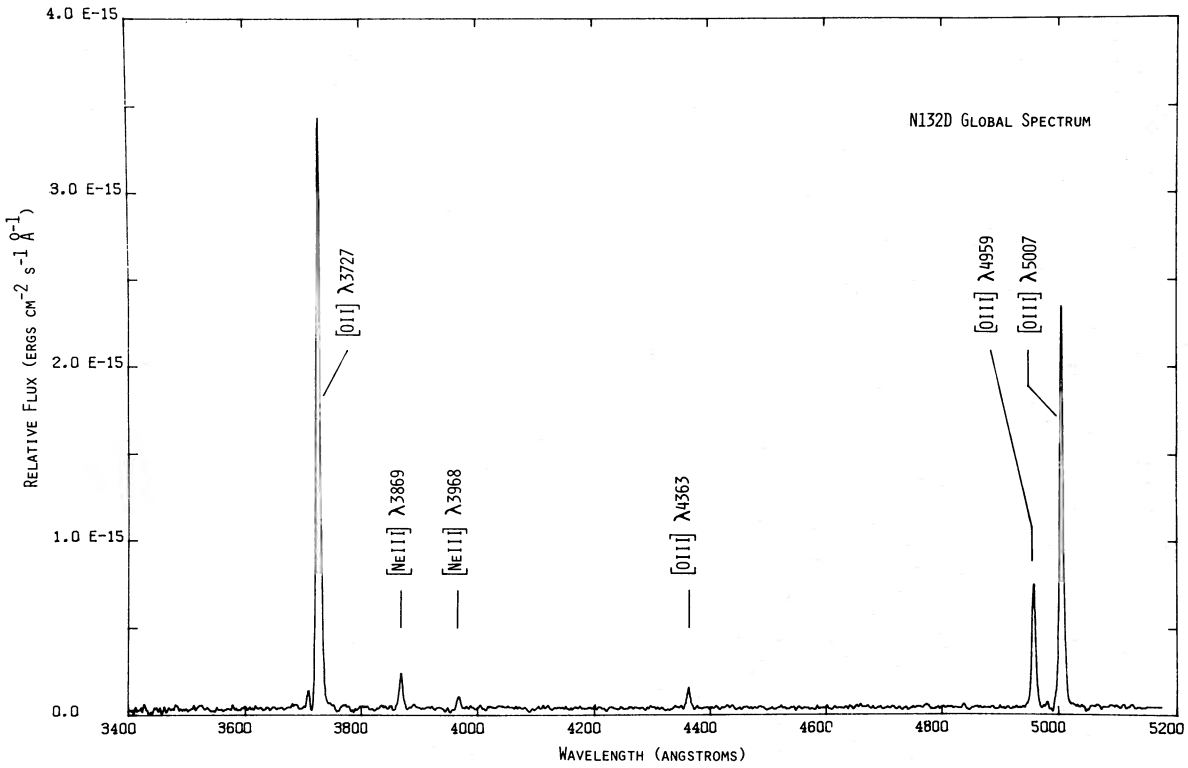

FIG. 2.—The moderate resolution global spectrum of N132D generated by the technique described in the text. The dip on the blue side of the [O II] λ3727 line is caused by imperfect subtraction of diffuse [O II] emission.

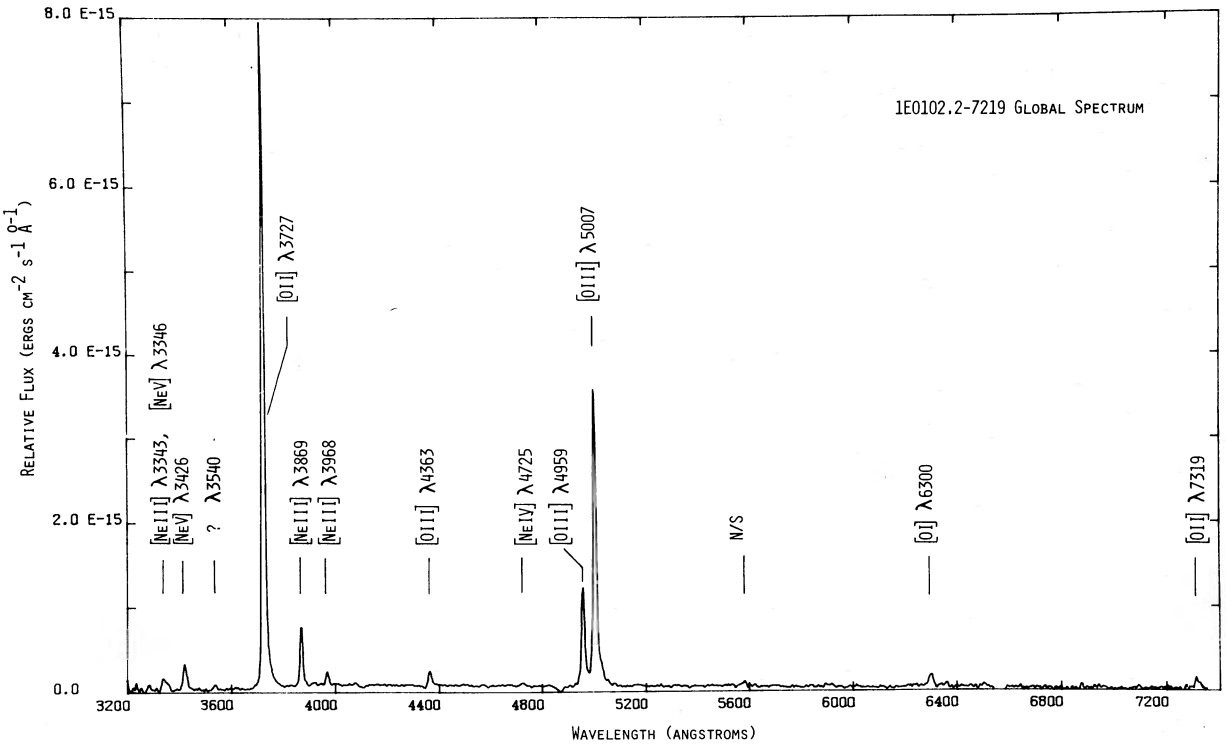

FIG. 3.—The global spectrum of 1E 0102 – 7219 generated by the technique described in the text. There is an unidentified emission feature near 3540 Å.

Weaver and Woosley (1980) and Woosley and Weaver (1981) have calculated the nucleosynthesis expected in a parameterized 25 $M_\odot$ Type II supernova. They find that elements lighter than silicon are made almost entirely by preexplosive nuclear burning and are pushed off the star when it explodes. Explosive burning of neon, oxygen, and silicon produces the elements heavier than silicon. The absence of emission of these heavier elements in N132D and 1E 0102.2−7219 suggests that the optically emitting material comes from outer (cooler) zones of the supernova explosions and will thus be composed of (in order of both abundances and mass fraction) oxygen, neon, carbon, magnesium, and silicon. Without a detailed model, no abundance limit can be placed on carbon relative to silicon, since the C II line at 4267 Å is a recombination line, whereas the lines of oxygen and neon are produced by collisional excitation. Silicon produces no important lines in the visible. Interesting limits might be obtained on the magnesium abundance from the absence of the Mg I] 4571 Å feature. If the zone containing Mg I also contained O I, then the ratio of the 4571 Å line and the 6300, 6363 Å lines would be in the ratio of the relative abundances of the elements multiplied by the ratio of the collision strengths and an exponential term, exp $[-8719/T_e]$. This would imply that in N132D and 1E 0102.2−7219, $N(\mathrm{Mg})/N(\mathrm{O}) \lesssim 0.03$. However, it is most probable that, owing to its lower ionization potential, Mg is mainly singly ionized in the neutral oxygen zone, in which case the ionization correction factor would be large, and no upper limit can be set on the magnesium abundance. Since even the upper limit with no ionization correction factor is consistent with the abundance ratio calculated by Weaver and Woosley (1980) and Woosley and Weaver (1981), we must conclude that our N132D and 1E 0102.2−7219 global spectra give no useful information on carbon, silicon, or magnesium abundances.

TABLE 4

VELOCITY DATA FOR THE BRIGHT LINES OF 0540−69.3[a]

IDENTIFICATION		MEASURED	VELOCITY FWHM	INFERRED V_r
Ion	λ(Å)	λ(Å)	(km s^{-1})	(km s^{-1})
[O II]	3727.5	3734.6 ± 1.0	1417 ± 45	573 ± 80
[O III]	4958.9	4969.5 ± 1.0	1400 ± 96	639 ± 60
[O III]	5006.8	5017.3 ± 0.8	1210 ± 30	637 ± 50
Ca I]	6572.8	6580.0 ± 3.0	1333 ± 45	332 ± 140
[S II]	6722.7[b]	6736.1 ± 2.0	1305 ± 43	597 ± 100

[a] Average of two measurements with slit running N-S and E-W through approximate center of remnant.

[b] Low density limit assumed for blend.

Among the spectra of Table 2 the LMC remnant 0540−69.3 is clearly outstanding, since there are no emission lines of neon, but both the blue and the red [S II] lines are strong (Fig. 4). In the context of the supernova models cited above, this immediately suggests that the optical emission originates from material ejected from the inner (neon-burnt) zones of the massive presupernova star, adjacent to the neutronized core. For a 25 $M_\odot$ Population I star, this material would contain Si, S, O, Ar, and Ca in order of abundance, which in the models, corresponds approximately to the 1.5–1.8 $M_\odot$ zone.

We now believe the feature which, in the discovery paper (Mathewson *et al.* 1980) was identified as [N II] λ6583 to be Ca I] for several reasons. In Table 4, we have collected data on peak wavelength, velocity dispersion, and inferred radial velocity for each of the bright lines in the spectrum. The data are derived from two 3000 s integrations of 1980 December (270 *R* grating) and 1981 November (250 *B* grating). For all lines, the measured velocity dispersions are in good agreement, and if we assume that the [S II] blend is near the low-density limit, the

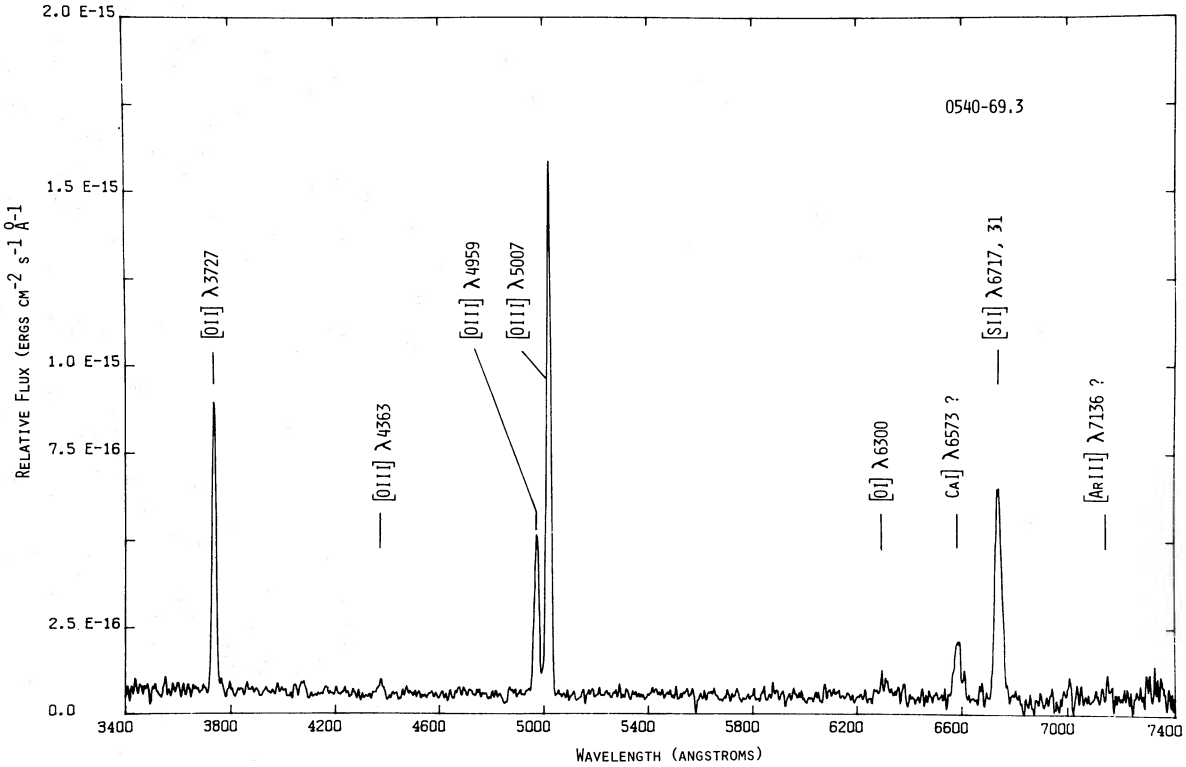

FIG. 4.—The spectrum of 0540−69.3 showing the absence of [Ne III] lines and the presence of [S II] and a feature near 6580 Å ascribed to Ca I]

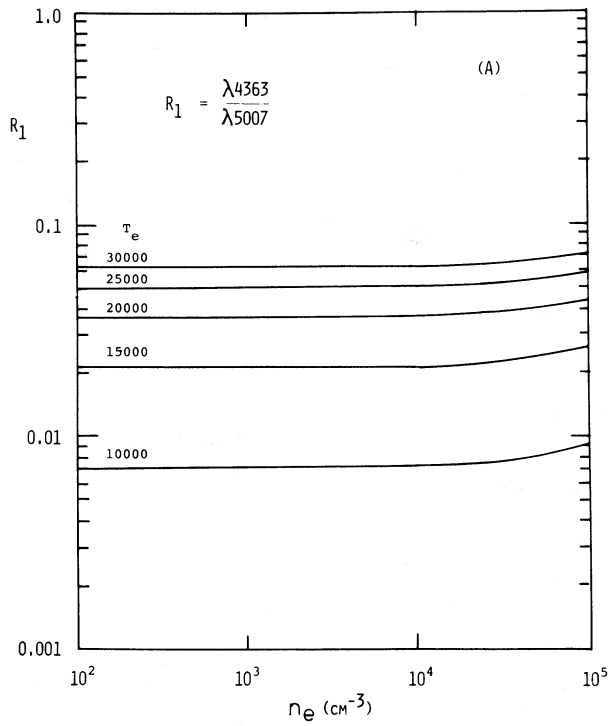

FIG. 5(*a*)

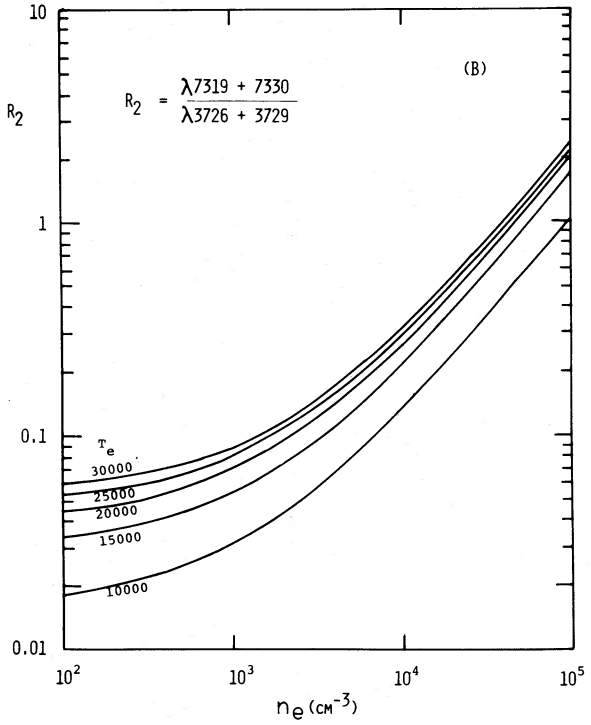

FIG. 5(*b*)

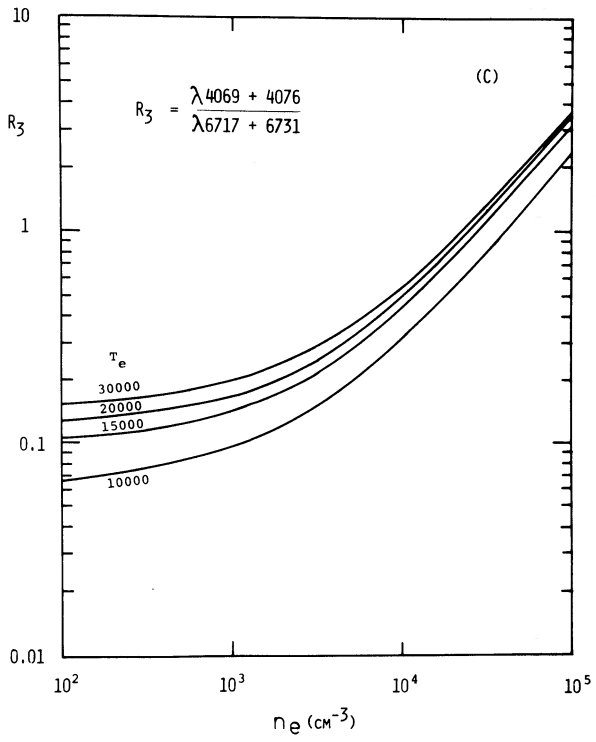

FIG. 5(*c*)

FIG. 5.—The temperature and density behavior of the diagnostic line ratios, R_1, R_2, and R_3 defined in the text.

radial velocity inferred for these lines is in good agreement with the oxygen lines. The feature at 6580.0 Å is likely to be either redshifted Hα, [N II], or the Ca I] $4s^1S$–$4p^3P^0$ line at 6572.78 Å. If it was [N II], we would expect a blueward asymmetry caused by the 6548.1 Å line. This is not seen in either of our spectra. Furthermore, the radial velocity inferred on the basis of an identification of [N II] 6583.4 Å would be -162 km s^{-1}, totally at variance with the other lines. If we assume an identification with Hα, then the radial velocity inferred, $+772$ km s^{-1}, would not be inconsistent. However, our spectrophotometry excludes the detection of Hβ at a level of 1.6 on the scale [O III] λ5007 = 100.0. This would imply a Balmer decrement of greater than 40. Reddening effects cannot decrease this by more than a factor of 2, since a steep Balmer decrement is not indicated in the surrounding H II region nebulosity. Such high Balmer decrements are not achieved in any astrophysical plasma, and this appears by itself to exclude the Hα identification. In any event, it would be very hard to imagine theoretically how either Hα or [N II] emitting gas could be mixed with, and share the expansion of, material ejected from deep within a massive star by a supernova event.

We strongly prefer the Ca I] identification. In collisional excitation of plasma which is predominantly un-ionized or in recombination of Ca II, the intercombination line would be the strongest Ca I feature in the visible. The next strongest would be the resonance lines at λ4575.45 Å and λ4226.73 Å, neither of which are seen. At such low ionization, there are no strong visible lines of the other species expected to be present (Si or Ar), except for, possible [Ar III] λ7135.8 Å. Our two spectra of 0540−69.3 do in fact show evidence for this line at a level of ~2.0 ([O III] λ5007 = 100.0).

If the feature near λ6580 is Ca I], this is consistent with the spatial distribution of calcium in the remnant. Direct imagery

of this feature through an interference filter centered at 6584 Å revealed that the SNR appeared as a ring of *smaller* diameter than the [O III] nebulosity (Mathewson *et al.* 1980). Since the 16 Å bandpass of the filter was well matched to the bulk of the nebular emission, we believe that little nebulosity has been lost by Doppler shifts larger than the bandwidth of the filter. This central concentration is therefore almost certainly real, and it is what would be expected from the Ca ejecta, which is concentrated in the zone close to the neutronized core in the supernova models.

III. PHYSICAL CONDITIONS

The derivation of physical conditions in the ejecta from the data given in Tables 2 and 3 is a very difficult, or, as we will show, an impossible task. The fundamental problem with these spectra is the scarcity of diagnostic line ratios. This remains true even if we adopt the drastic simplifying assumption that common physical conditions apply to the emission zones of all the ionic species observed. From the observed spectra, only three ratios can be defined which are independent of both chemical abundance and ionization conditions. These are $R_1 = \lambda 4363/\lambda 5007$ Å, $R_2 = \lambda 7319 + 7330/\lambda 3726 + 3729$ Å, and $R_3 = \lambda 4069 + 4076/\lambda 4617 + 6731$ Å, applicable to the O III, O II, and S II ions, respectively. These ratios have been computed from a five-level atom approximation for each ion, accounting for all collisional and radiative processes between levels. The atomic data used were taken from the compilation of Mendoza (1983). The computed values of R_1, R_2, and R_3 are given as functions of electron temperature, T_e, and electron density, n_e, in Figures 5*a*–5*c*.

A simultaneous solution for R_1 and R_2 indicates (in all objects) that we are in a high-temperature/low-density regime. Ignoring any reddening corrections, this direct solution gives for each object (T_e, n_e): G292.0+1.8 (20,000, 2500); 0540−69.3 (18,000, $\lesssim$100); N132D (23,000, $\lesssim$100); 1E 0102.2−7219 ($\sim$23,000, $\lesssim$100). No solution would be possible in the cases of 0540−69.3 and N132D if there was any appreciable reddening. For a "standard" reddening curve (e.g., Kaler 1976), the maximum logarithmic reddening constant allowed in the case of G292.0+1.8 would be 0.45, in which case the solution gives (22,000, $\lesssim$100).

We have little confidence in any of these solutions, however, since the result in 0540−69.3 is inconsistent with the solution for the S II zone found from the ratio R_3 and the density-sensitive λ6731/6717 Å ratio. This gives (7000, 2000) with large error. Our assumption that common physical conditions apply to zones of different ionization is therefore at fault. This implies that, not only are our estimates of the physical conditions very crude, but also that any attempt to use these to derive relative abundances will lead to rather gross errors. This observational situation applies to all previous optical work on this type of supernova remnant, and improvements must await an extension of the wavelength baseline into the near-infrared and (more importantly) the ultraviolet.

In the absence of further observational data, some progress possibly could be made by constructing a plausible physical model for the line-emitting region. In the companion paper (Dopita, Binette, and Tuohy 1984), we examine the shock hypothesis that has usually been advanced as the cause of the optical emission. In this model, radiative shocks are supposed to be moving into dense knots of ejecta during the reverse-shock phase of the SNR evolution.

IV. CONCLUSIONS

From our spectrophotometry of four oxygen-rich SNRs in three galaxies, we find surprisingly little variation in excitation conditions as evidenced by either the [O III] temperature or the [O I]/[O II]/[O III] line ratios. Unlike the extraordinary remnant in NGC 4449 (Blair, Kirshner, and Winkler 1983), densities are sufficiently low that collisional deexcitation effects appear to be negligible. Although we have shown that the optical data are insufficient to derive a unique set of physical conditions in the filaments, we believe that the similarity in line ratios is a consequence of a common physical process operating in all four SNRs.

For three of the remnants, the similar ratio of [Ne III]/[O III] lines suggests that the Ne/O abundance ratio does not vary greatly and that material having its origin in helium-burnt zones of the precursor star is presently emitting in optical frequencies. However, the LMC remnant 0540−69.3 is anomalous in its composition. Here, we appear to be observing neon-burnt material originating from close to the neutronized core in which oxygen, sulfur, and calcium emissions are dominant.

We thank Don Mathewson and Vince Ford for their assistance in acquiring some of the data reported herein, and we acknowledge the excellent support provided by the staff of the Anglo-Australian Observatory.

REFERENCES

Balick, B., and Heckman, T. 1978, *Ap. J. (Letters)*, **226**, L7.
Blair, W. P., Kirshner, R. P., and Winkler, P. F. 1983, *Ap. J.*, **272**, 84.
Boksenberg, A. 1972, *Proc. ESO/CERN Conference on Auxiliary Instrumentation for Large Telescopes*, Geneva, May 2–5, p. 295.
Chevalier, R. A., and Kirshner, R. P. 1978, *Ap. J.*, **219**, 931.
———. 1979, *Ap. J.*, **233**, 154.
Danziger, I. J., and Dennefeld, M. 1976*a*, *Pub. A.S.P.*, **88**, 44.
———. 1976*b*, *Ap. J.*, **207**, 394.
Dopita, M. A., Binette, L., and Tuohy, I. R. 1984, *Ap. J.*, **282**, 142.
Dopita, M. A., Tuohy, I. R., and Mathewson, D. S. 1981, *Ap. J. (Letters)*, **248**, L105.
Goss, W. M., Shaver, P. A., Zealey, W. J., Murdin, P., and Clark, D. H. 1979, *M.N.R.A.S.*, **188**, 357.
Kaler, J. B. 1976, *Ap. J. Suppl.*, **31**, 517.
Kamper, K., and van den Bergh, S. 1976, *Ap. J. Suppl.*, **32**, 351.
Kirshner, R. P., and Blair, W. P. 1980, *Ap. J.*, **236**, 135.
Kirshner, R. P., and Chevalier, R. A. 1977, *Ap. J.*, **218**, 142.
Lasker, B. M. 1978, *Ap. J.*, **223**, 109.
———. 1980, *Ap. J.*, **237**, 765.
Mathewson, D. S., Dopita, M. A., Tuohy, I. R., and Ford, V. L. 1980, *Ap. J. (Letters)*, **242**, L73.
Mendoza, C. 1983, in *IAU Symposium 103, Planetary Nebulae*, ed. D. R. Flower (Dordrecht: Reidel), p. 143.
Murdin, P., and Clark, D. H. 1979, *M.N.R.A.S.*, **189**, 501.
Oke, J. B. 1974, *Ap. J. Suppl.*, **27**, 21.
Peimbert, M. 1971, *Ap. J.*, **170**, 261.
Tuohy, I. R., and Dopita, M. A. 1983, *Ap. J. (Letters)*, **268**, L11.
van den Bergh, S., and Dodd, W. W. 1970, *Ap. J.*, **162**, 485.
Weaver, T. A., and Woosley, S. E. 1980, *Ann. NY Acad. Sci.*, **336**, 335.
Woosley, S. E., and Weaver, T. A. 1981, in *Essays in Nuclear Astrophysics*, ed. C. A. Barnes, D. D. Clayton, and D. N. Schramm (Cambridge: Cambridge University Press), p. 377.

M. A. DOPITA and I. R. TUOHY: Mount Stromlo and Siding Spring Observatories, Private Bag, Woden, P.O. ACT 2606, Australia